NBSIR 83-2645 (FDA)

Characterization of Porosity in Porous Polymeric Implant Materials

U.S. DEPARTMENT OF COMMERCE
National Bureau of Standards
Dental and Medical Materials
Polymer Science and Standards Division
Washington, DC 20234

February 1983

Annual Report for period April thru September 1982

Prepared for:
Office of Medical Devices
National Center for Devices and Radiological Health
Food and Drug Administration
Silver Spring, MD 20910

NBSIR 83-2645 (FDA)

CHARACTERIZATION OF POROSITY IN POROUS POLYMERIC IMPLANT MATERIALS

R. E. Dehl

U.S. DEPARTMENT OF COMMERCE
National Bureau of Standards
Dental and Medical Materials
Polymer Science and Standards Division
Washington, DC 20234

February 1983

Annual Report for period April thru September 1982

Prepared for:
Office of Medical Devices
National Center for Devices and Radiological Health
Food and Drug Administration
Silver Spring, MD 20910

U.S. DEPARTMENT OF COMMERCE, Malcolm Baldrige, *Secretary*
NATIONAL BUREAU OF STANDARDS, Ernest Ambler, *Director*

TABLE OF CONTENTS

FIGURES

ACKNOWLEDGMENTS

The author is indebted to a number of members of the Dental and Medical Materials Group for their assistance in this work; to Dr. S. Venz, a guest worker from the Free University of Berlin, for her assistance in performing the compressive stress-strain measurements; to Mr. J. E. McKinney for his suggestions about the resin and polishing methods used in preparing samples for optical microscopy, to Dr. R. L. Bowen for suggesting the dye used to color the resin, and to Dr. W.-L. Wu for the use of the microscope and camera in the optical analysis work.

The author is also grateful to Professor E. E. Underwood of the Georgia Institute of Technology, a well-known authority in quantitative microscopy, for his valuable suggestions about the optical analysis of filled porous polyethylene.

ABSTRACT

In this report, we describe (1) the continued exploration of methods for characterizing the porosity of two commercial implant materials, a porous polyethylene and a composite of polytetrafluoroethylene and carbon, and (2) the compressive stress-strain behavior of these materials. A major emphasis was placed upon optical image analysis of porous polyethylene. The pore volume fraction (0.47) obtained from analysis of 20 photomicrographs agreed well with the fraction previously found by two other methods. The mean intercept length, determined from the same photomicrographs, was about 75 μm, a value considerably higher than the average "interconnecting" pore diameter determined by mercury porosimetry (30 μm). Replotting our mercury porosimetry data, we found that the volume-weighted pore size distribution curve resembled a log-normal distribution, skewed to the right of the "most probable" pore radius. The surface area determined from mercury porosimetry data was somewhat larger (0.125 m^2/g) for the porous polyethylene than that determined by the BET method (0.082 m^2/g), while the reverse was true for the composite material (0.19 vs 0.45 m^2/g). Compressive stress-strain measurements on the laminated composite demonstrated that the initial compression modulus is approximately six times greater when the stress is applied parallel rather than perpendicular to the laminar planes.

I. INTRODUCTION

The rationale for this project and the approaches to be used in characterizing the porosity of porous polymeric implant materials have been discussed in previous Annual Reports to the Bureau of Medical Devices (FDA)[1,2]. During the current half-year reporting period (Apr. 1, 1982 - September 30, 1982), we were guided by a work plan which was drafted by mutual agreement between staff members of the Bureau of Medical Devices and the National Bureau of Standards. It was agreed at the time the work plan was drafted that the 7 items in the plan likely would require a greater effort than could reasonably be expected, given the available resources, in half a year. We therefore were faced with a choice about how to apportion the available time. We could either make a thorough investigation of 2 or 3 items in the plan, or attempt to make some progress on most or all of the tasks. The latter approach was chosen, because we thought it important to pass the exploratory phase of this work as soon as possible. In this way, we could lay the foundation for future investigations, with enough knowledge about each of the porosity characterization methods to have a rational basis for selecting the most appropriate one(s) for any given problem that we might encounter. In retrospect, we believe that this was a wise choice. We believe that we now have the expertise to perform each of the tasks specified in our work plan and that future acquisition and interpretation of data will be limited largely by time and resources.

In accordance with the priorities assigned to the items in our work plan, we have placed more emphasis on optical image analysis than on some other methods which were investigated last year. This emphasis has culminated in some very encouraging experimental results, as discussed

in Section IID. In addition, progress was made in corroborating our surface area measurements of last year according to the BET method, so-named for the initials of its inventors[2]; in establishing another method for measuring surface area; in measuring the limits of mechanical stress which should be applied to the porous materials; and in understanding how to plot mercury porosimetry data in order to extract the maximum information from such data.

The two porous implant materials which are discussed in this report are Plastipore[3]® and Proplast[4*]®. The former is a porous polyethylene (PPE), and the latter is a composite of polytetrafluoroethylene (PTFE) and carbon (C).

II. POROSITY MEASUREMENTS BY QUANTITATIVE MICROSCOPY

Several books[5-9] have been written about the inference of 3-dimensional structures from the examination of 2-dimensional planar cross-sections of particulate or multiphase materials. The methods have been applied extensively to metal alloys, ceramics, biological tissues, and powdered materials, as well as to porous polymers. A science of "stereology" has developed to treat the various types of information which can be derived from 2-dimensional analysis of solid materials, with a standardized system of nomenclature developed by the International Society for Stereology. In the following discussion, we will define the few symbols needed to describe our measurements for pore size and pore volume, as measured on planar cross-sections of the material.

*Certain commercial materials and laboratories are identified in this report in order to specify experimental procedures adequately. In no case does such identification imply recommendation or endorsement by the National Bureau of Standards, nor does it imply that the identified materials or laboratories are necessarily the best available.

A. Pore Volume

The symbols needed for these discussions are V, A, L and P, which stand for volume, area, length, and points, respectively. A fraction, such as the volume fraction of voids in a solid material, is represented by the symbol V_V, which stands for volume (of voids)/total volume. The equations which allow us to infer 3-dimensional information about void volume from planar cross-sections of the material are very simple, quite general, and independent of any weakening assumptions about shape, size, or spatial distribution of pores in the solid. In all cases, they represent a statistical average of a large number of measurements. In the fractional notation, they are (e.g. Ref. 5, Chap. 3):

$$V_V = A_A = L_L = P_P \qquad (1)$$

The volume fraction of voids (V_V) which we want to know, is the same as the area fraction in 2 dimensions (A_A) and the one-dimensional intercept length fraction of total length (L_L), for random lines drawn on the 2-dimensional surface. The fraction P_P is derived by placing a transparent grid of crossed lines on the photomicrograph. Each line intersection is called a "point" and the number of these points falling within the regions of interest, divided by the total number of intersections, is P_P. For ambiguous points which may or may not lie in the region of interest, one assigns the value 1/2, because on the average, over a large number of counts, such points will lie in this region 50 percent of the time. From these equations, we see that there are 3 different ways to measure void volume on a planar cross-section. The point-count (P_P) method is generally found to be the easiest to perform by manual methods. Of course, one such point count is not a good measure of V_V, and if the sample is anisotropic, one cross-section may not be an adequate sampling.

A method for estimating the sample size necessary to achieve a given level of accuracy is given in Section IIC.

B. Pore Size

1. General Considerations

As we have stated previously, the "size" of irregularly shaped objects such as the pores in implant materials is not a well defined physical property. The only pore shape which can be treated rigorously by stereological methods is the sphere. We will discuss this case in some detail, because it illustrates the method by which, in principle at least, any pore "size" may be deduced by 2-dimensional stereological analysis.

We imagine a solid material having spherical holes randomly distributed throughout. For simplicity, we assume that all the holes have the same diameter D, although it is also possible to deduce the distribution of spherical pore diameters, if more than one is present, by stereological methods. If we slice through the porous solid, we will see circles on the surface of the cross-sections which result from random sectioning of the spheres, and the diameters of these circles will range from 0 to D. Obviously, the average diameter of these circles will be less than D, whereas the average diameter of the spherical holes, which we want to know, is exactly D. If we examine a very large number of cross-sections, we will occasionally see a circle which has a diameter very close to D, so that one way to estimate D would be to look at a great many cross-sections and find the largest circle. However, this method is relatively inefficient, and one could never be sure that the next section would not reveal a D larger than any found previously. A more efficient way to converge on the desired answer with fewer cross-

sections is to use all of the data, i.e., all of the measured diameters obtained in each cross-section. A straightforward geometrical analysis[7] shows that the average diameter obtained in this way ($\overline{d}$) is related to the spherical diameter D by the relationship

$$\overline{d} = \pi/4\ D. \tag{2}$$

Instead of measuring the diameters of all the circles, one may measure the average chord length $\overline{l}$, obtained by drawing lines at random across the cross-sections. The average chord length will be less than $\overline{d}$, because only chords which happen to pass through the center of the circles will be equal to d. In fact, it is easily shown that $\overline{l}$ is related to $\overline{d}$ by the relationship

$$\overline{l} = \pi/4\ \overline{d}. \tag{3}$$

From Eqs 2 and 3, we find that

$$D = (4/\pi)^2\ \overline{l} = 1.62\ \overline{l} \tag{4}$$

In other words, we can deduce the diameter of the spherical pores in the solid by measuring the average intersected chord lengths in one dimension.

Although derived for spherical pores, Eqs. 2, 3 and 4 apply equally well to irregularly shaped pores, if we remember that we are not measuring a true "diameter" when the shapes are irregular. In such cases, the D which one finds by measuring cross-section "diameters" or chord lengths is a parameter which may be thought of as an equivalent pore diameter, or the diameter which one would determine if the pores were spherical in shape.

The methods described above for measuring pore diameters and chord lengths might appear to be prohibitively time-consuming and tedious, requiring the use of rulers and calipers to measure the lengths, and a computer to store and process the data. We must seek ways of measuring

these "size" parameters which can be more easily performed. Two principles are a guide to finding a more suitable method:

(1) Since we are limited to manual, rather than instrumental, methods of analysis, we seek methods which are as simple and rapid as possible, in order to produce a statistically significant amount of useful data in a reasonable time.

(2) The methods should also be as objective as possible, requiring a minimum of operator judgment in making the measurements. In this way, one hopes to select methods by which different researchers will obtain essentially the same results for the same materials.

In theory, a third criterion should be added to these 2, namely that the method should measure aspects of pore shape as well as size, since these are undoubtedly related to the tissue ingrowth process. Unfortunately, we do not know how this process is affected by pore shape, so that we really do not know what "shape factors" to measure. Even if we did know this, the measurements of shape (pore contours, tangent diameters, etc.) would require the use of at least semi-automatic instrumentation for measuring such quantities and storing the data. Manual methods would be prohibitively time-consuming.

Fortunately, there is at least one objective and relatively easy way to measure pore "size" manually by optical image analysis. It yields the so-called "mean intercept length", $\overline{L}$.

2. Mean Intercept Length

The mean intercept length is defined as the average length of all possible chords intersecting the pores, for all possible lines drawn through the sample. Fortunately, it is not necessary to use rulers or calipers in order to make this measurement. The task is reduced to a

simple counting procedure on sample cross-sections by one of the basic stereological relations[7],

$$\bar{L} = P_P/N_L, \qquad (5)$$

where P_P is the point count fraction of the desired phase, described above, and N_L is the number of chord lengths for that phase per unit test length. This equation is readily constructed if we remember (Eq. 1) that $P_P=L_L$. The average intercept length is just the total intercept length L_L for a given test line, divided by the number of intercepts in that line, N_L. The method is illustrated below:

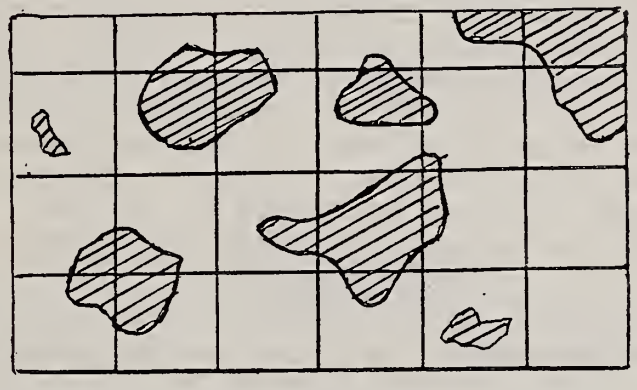

Here, we have placed a 3 x 5 line transparent test grid on a photomicrograph of a planar cross-section of a 2-phase solid. If we are interested in measuring $\bar{L}$ for the shaded phase, we first measure P_P. There are 3 out of 15 intersections which lie in the shaded phase regions, so that P_P = 3/15 = 0.2. The number of intercept chords N for the horizontal lines is 5 1/2, where the fractional count comes from the intercept in the upper right corner which only traverses part of that cut-off area. Over a large number of counts, these partial chords will average to half the actual chord lengths which one would measure if the entire area were visible. In the same way, we find that N for the 5 vertical lines is also 5 1/2. Thus, N_L for all the lines is 11 divided by the total test length L. We have calibrated the test grid by photographing a ruled

graticule, by which we found that 1 cm of test line in the photograph equals 20 μm of sample length. The total length of test lines, horizontal and vertical, is 50 cm, or 1000 μm of sample length. Therefore, N_L = 11/1000 μm, and $\bar{L} = P_P/N_L$ = 18 μm.

This method is relatively efficient, because the same overlay grid can be used to measure P_P and N_L. Unfortunately, we must make a large number of such measurements in order to obtain a good statistical average. The estimation of sample size is described in the following section.

C. Statistical Analysis and Prediction

It is important to be able to estimate the number of measurements needed to achieve the desired degree of accuracy in our stereological analysis. The equation which defines this required number (N) of measurements is quite general[5]. It may be written in the form

$$N = \left[\frac{SD(100)s(x)}{(\%acc.)m(x)}\right]^2, \qquad (6)$$

where x is the measured quantity (e.g., P_P for our volume fraction measurement), m(x) and s(x) are the sample mean and standard deviation, respectively, SD is the number of standard deviations desired, and the percent accuracy (% acc.) is defined as the half width of the chosen confidence interval divided by the mean. It may be assumed that $\mu(x) \cong m(x)$ and $\sigma(x) \cong s(x)$, where μ and σ represent the population (or true) mean and standard deviation, and m and s are for one large sample taken from the population. (A sample of at least 30 is recommended to give a reasonable estimate of μ and σ). Having determined m and s, we can use Eq. 6 to estimate N.

Because N varies inversely with the square of the percent accuracy, it may be necessary to compromise this latter quantity somewhat in order to keep the number of measurements within reason. Of course, one can

arbitrarily decide on a reasonable N and accept the percent accuracy and/or the confidence interval required to satisfy Eq. 6.

D. Optical Analysis of Porous Polyethylene

Porous polyethylene was selected as the first material to be examined by stereological techniques, rather than the PTFE-C composite. The latter has a more complex morphology than PPE, due in part to the fact that there are 3 phases present, and it was decided that our experimental procedures should be developed and tested on the less complex material.

1. Sample Preparation

Two criteria must be met in preparing a sample for analysis by optical microscopy. First, the surface of the specimen must be flat and smooth, so that each sample area can be brought entirely into the focal plane of the microscope. Second, there must be sufficient light or color contrast between the different phases so that they can be clearly differentiated. The first criterion was easily achieved for the PPE, but the second proved to be somewhat more difficult.

It was not possible to polish unfilled PPE to give a smooth surface, due to the softness and elasticity of the material. Rather, it was necessary first to fill the pores with a matrix material which became hard enough to provide the necessary sample rigidity for grinding and polishing. For this purpose, we used a clear polyester resin[10] which hardens upon addition of a small amount of peroxide initiator. The curing rate of this resin-peroxide mixture was sufficiently slow to permit the PPE to imbibe the liquid to a depth of about 1 mm before the penetration stopped. After the resin was sufficiently hard (about 1-2 days), the filled samples

were polished with graded carborundum papers (minimum roughness 600 grit), followed by polishing with 0.05 μm alumina powder.

2. Photomicrography

A typical photomicrograph of polished, filled PPE using overhead (direct) illumination is shown in Fig. 1(a). The pictures were taken with a Polaroid ® camera attached to the microscope, using type 52 medium contrast positive film. Careful examination of this photograph reveals that there is probably more than one phase present; however, the contrast is not sufficient to permit quantitative measurements to be made. After a number of unsuccessful attempts, we discovered a dye, Sudan B Black, which was soluble in the liquid resin, did not inhibit the curing process excessively, and yet provided enough light contrast to outline the phase boundaries. A typical photomicrograph of the PPE filled with the dyed resin is shown in Fig. 2b.

The photographs are inferior in quality to the direct visual image as seen through the stereo eyepieces. Ideally, therefore, one should perform the stereological analysis directly on the visual image rather than on photographs. However, direct visual methods also have some drawbacks, particularly if one wishes to make a large number of measurements. They require intense operator attention, leading to rapid fatigue, because one cannot use a pointer as on a photograph to keep track of the linear traverses. Any distraction necessitates a recount. There is also an obvious advantage in having a hardcopy record of the images for future reference. For these reasons, we chose to use the photograhic method of image analysis.

The stereological measurements were performed using a 6 x 4 line test grid overlay scribed on transparent film. The choice of grid

a

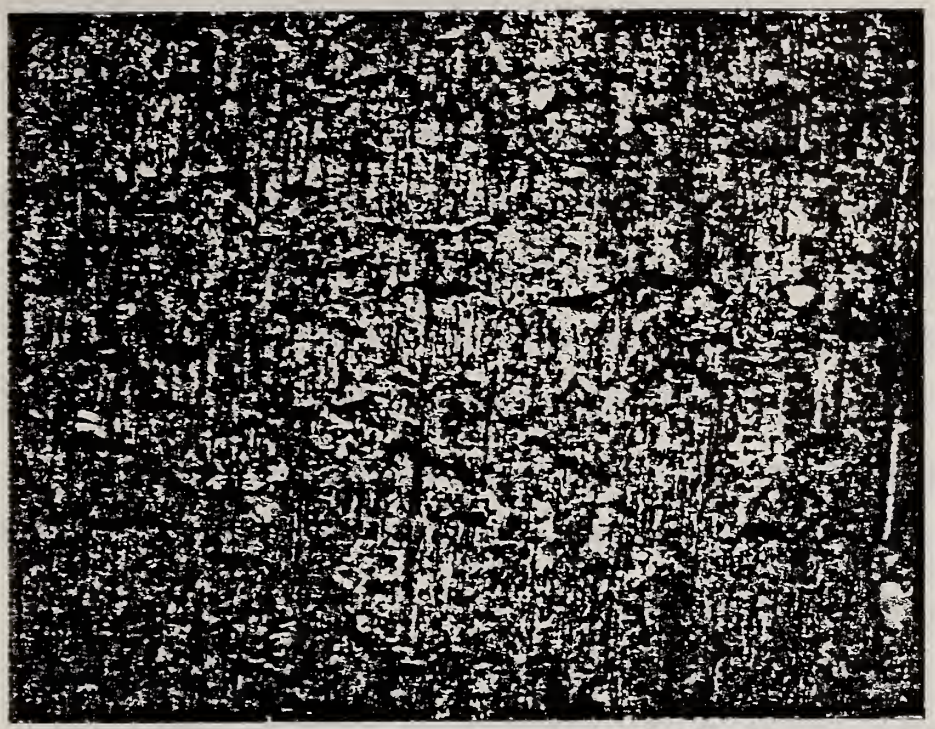

b

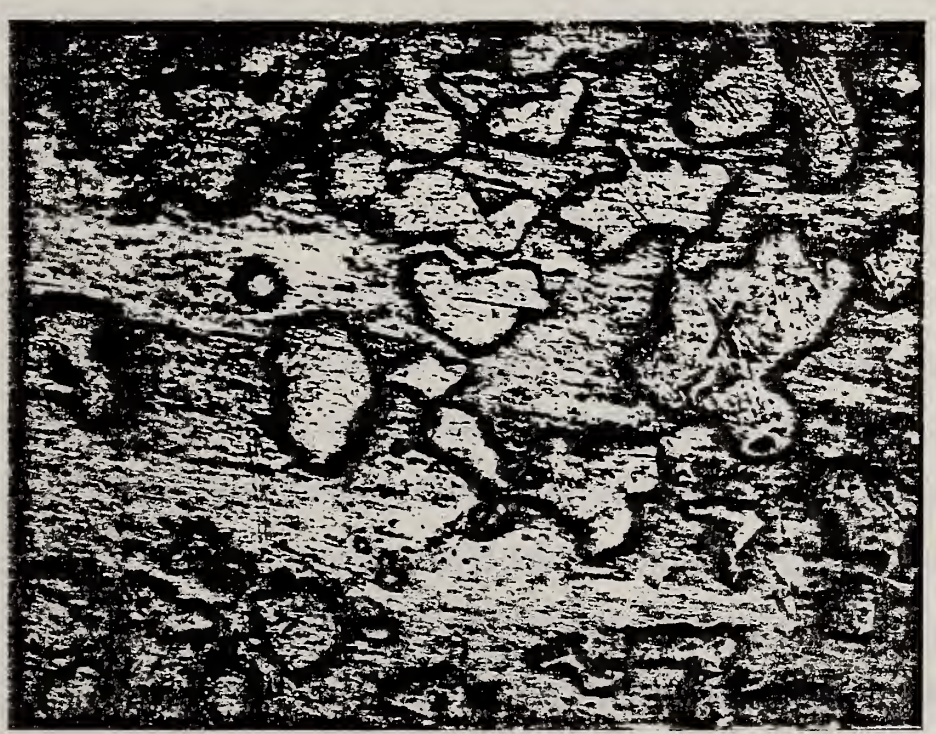

Figure 1. Photomicrographs of polished cross-sections of filled porous polyethylene; (a) resin undyed, (b) resin dyed. One polyethylene "blister" marked X.

spacing is not a critical matter, but as a rule it is well to avoid spacings which are very large or small as compared with the size of the regions of interest in the photomicrograph. If the grid spacing is too small, time and effort are wasted in counting many adjacent points lying in the same phase region. If the spacing is too wide, one discards a great deal of available information in the photograph. Similarly, the microscope magnification was chosen to give photographic images which allowed us to distinguish the phases easily but were not so enlarged as to contain very few phase regions.

At first sight, Fig. 1(b) may not appear to offer enough phase contrast to differentiate the 2 types of phase regions. The visual image, however, allowed us to make this distinction and provided the clues necessary to permit quantitative analysis. A careful examination of the photograph reveals that one phase seems to consist of slightly raised areas or "blisters", elevated above the other phase. Apparently, during the grinding and polishing of the sample, one of the phases lagged slightly behind the other as the wear proceeded. The question of which phase was which, while not obvious from the photographs, was resolved by close examination of the visual image. The lower (non-raised) phase was seen to contain many small bubbles, as one would expect in a cured resin but not in the polyethylene. We therefore assumed that the lower areas represent the filled pores, and it was this phase that was measured stereologically.

3. Results

Two sets of 10 photomicrographs each were taken on randomly selected areas of one sample of filled, polished PPE. The 2 sets were taken

under somewhat different conditions. For the first set, a 10X microscope objective was used in combination with a 10X camera projection lens. The exposure times were rather long (90 s), and we took the other set of photographs using a 20X objective and 4X projection lens which shortened the exposure to 11 s. The photographic magnification was adjusted in each case by raising or lowering the camera bellows. The magnification was measured by photographing a ruled graticule graduated in 10 μm increments. In this way, the two sets of photographs were found to have magnification ratios of 5.7 and 6.9 μm (sample)/mm (photograph).

The results obtained for the pore volume fraction (P_p) and mean intercept length ($\overline{L}$) for the 2 sets of photomicrographs are given in Table 1. Despite the wide range of values obtained within each set of photographs for both P_p and $\overline{L}$, the 2 sets are in very close agreement with respect to all 4 properties reported in Table 1. All of the photographs were used; none was discarded because it appeared less clear or less "typical" than the others. This procedure was intended to minimize possible bias in the measurements due to subjective selection of the data.

Even a casual inspection of the various photographs revealed that there was indeed quite a wide variation in pore volume fraction and intercept lengths for the different sampled areas. In other words, the surface was not at all homogeneous on the dimensional scale of the areas sampled in these photographs. Many more measurements should be made on these and other samples of filled PPE in order to establish confidence in the measured values of P_p and $\overline{L}$.

Table 1: Optical Microscopic Measurements of Porosity in Porous Polyethylene

Volume Fraction of Pores (P_p)

10 Photographs	Mean	Std. Deviation	High	Low
Set 1	0.48	0.09	0.58	0.37
Set 2	0.46	0.07	0.54	0.33

Mean Intercept Length (μm)

10 Photographs	Mean	Std. Deviation	High	Low
Set 1	74	18	99	44
Set 2	76	15	97	48

III. PORE SIZE DISTRIBUTION BY MERCURY POROSIMETRY

In our last Annual Report[2], we have discussed the use of mercury intrusion porosimetry to measure both the pore volume and the pore size distribution in the porous implant materials. Briefly, the technique consists of forcing mercury into an evacuated sample of the material with applied pressure and measuring the volume of intruding mercury as a function of pressure. There is an inverse relation between the pressure and pore "diameter". The latter is strictly defined only for circular cylindrical pores, for which the equation relating diameter (D) to pressure (P) was found by Washburn[11] to be

$$PD = -4\gamma\cos\theta,$$

where γ and θ are, respectively, the surface tension of mercury and its contact angle on the material of interest. When the pores are of irregular shape, as in the porous implant materials, the quantity D may just be considered a parameter related to the average size of the interconnecting pores in the matrix.

Mercury porosimetry appears to be the only technique by which a distribution of pore "diameters" can easily be obtained, and for this reason it is important to consider how best to plot the data in order to extract the maximum amount of useful information from it. As a first approximation, the distribution can simply be plotted as a bar graph of void volume fraction vs pore size range. This procedure was illustrated in Ref. 2, page 17. For some purposes, this type of plot may be sufficiently detailed to contain all the desired information. However, it is possible to make a more detailed plot, as discussed in the following sections.

The question of the distribution of pore "sizes" depends in part upon the kind of information desired. There are at least two ways to describe a distribution of pore sizes:

(1) Distribution of pore volumes or volume-weighted pore size distribution. In this case, a given range of pore "diameters" is plotted vs. the volume fraction having this pore size range.

(2) Distribution of pore "diameters". In this case, a given range of pore diameters is plotted vs. the number fraction of pores having these diameters.

While either of the above could be a useful way of characterizing the pore size distribution, (1) is the only one that can be obtained directly from mercury intrusion data. It might be argued that the volume-weighted distribution is the more meaningful of the two in terms of tissue ingrowth. For example, if one is interested in the pore size range 50-100 μm for tissue ingrowth, it would seem to be more useful to know that 30% of the total pore volume has this "diameter" range than simply to know that a certain fraction of all the pores lie within this

range of diameters. For the anchoring of these materials by tissue ingrowth, it is surely not only the diameter of the pores but also the volume of pores to be filled with tissue that is important.

A. Instrumental Sensitivity

There is a problem in obtaining a very well defined plot of pore size vs. pore volume from mercury porosimetry data, due to the fact that the sensitivity of a porosimeter as a pore size measuring device varies over any given pressure range, and it is especially poor in the size range corresponding to large pores. For example, the range of ΔP from 0-1 psia corresponds to a pore "radius" range from 116 μm-∞, whereas same ΔP in the range 4-5 psia corresponds to 23-29 μm pores, and the range 14-15 psia corresponds to a radius range of only 7.7 - 8.0 μm. Clearly, the sensitivity of a mercury porosimeter as a pore-size measuring device increases rapidly with increasing pressure. It is, in fact, not possible to obtain detailed information about pore sizes below about 1.5 psia (80 μm pore radius and up) because P and V cannot be read with sufficient precision.

B. Random Error Analysis

It is useful to begin the discussion of pore size distribution by estimating the random errors in the mercury intrusion experiment, and it is emphasized that this analysis pertains only to random errors. Systematic errors of unknown magnitude are also present, and they have been discussed in our last Annual Report[2]. The volume of intruded mercury (V) can be estimated on the dilatometer stem to about ± 0.001 cm^3 (± 1 μL). This range of ΔV corresponds to a ΔP of about ± 0.05 psia near the low end of our P-V plot. Because the slope of the P-V curve varies considerably over its course, the ΔP corresponding to a given ΔV also varies. In

addition, there is an estimated uncertainty of about ±0.02 psia in reading the pressure gauge. There is also a small uncertainty due to the tendency of both the mercury column and the pressure gauge to "stick" slightly. All together, these effects appear to add up to random error limits of about ±0.1 psia for any P corresponding to a given V.

C. Volume-Weighted Pore Size Distributions

In order to construct a volume-weighted pore size distribution plot from mercury porosimetry data, we start with a volume vs pressure plot of the data obtained in a single mercury intrusion experiment. Examples of these s-shaped curves were given in our last Annual Report (Ref. 2, pp 15, 18, 19). Reading directly from these plots, we make a table of ΔV corresponding to each ΔP increment, from P = 0 to the maximum applied pressure. Our choice of ΔP is guided in part by the above random error analysis, which indicates that we are not justified in choosing $\Delta P < 0.2$ psi, due to uncertainties in the measurement. Of course, ΔP may have any value larger than 0.2 psi, and it does not need to be constant over the entire curve. We could then make a histogram plot of ΔV vs P, using our chosen interval width(s) for ΔP. However, what we really want to know is the void volume fraction $\Delta V/V_T$, where V_T is the total volume, which corresponds to each pore radius interval Δr.

From the Washburn equation, we know that r varies inversely with P, so that a plot which is linear with respect to r will not be linear with respect to P. It is impractical to try to plot $\Delta V/V_T$ vs a constant Δr, even though this is the desired histogram, because of the problem of varying sensitivity discussed above. A Δr which corresponds to a measurable ΔV near the low pressure end of the P-V curve would be much too large near the high pressure end, where it would correspond to a

large fraction of the total pore volume and obscure much of the desired details of the histogram. However, this difficulty is easily overcome, either by using a variable Δr or a constant or variable ΔP. A constant ΔP usually seems to cause an appropriate variation of Δr automatically, because of the inverse relationship. In Fig. 2a we have plotted a histogram of $\Delta V/V_T$ (%) vs. r, using a constant ΔP = 0.5 psi, for one sample of the composite material. This histogram has increasing radius interval widths, reading from left to right, which is a graphical demonstration of the decreasing accuracy of mercury porosimetry data as P decreases (or r increases). Note that the step widths are so small at the left end of the plot that one cannot read off Δr directly from the plot.

Clearly, Fig. 2a would be more useful if the radius interval widths were constant across the plot. In this way we could, for example, easily compare the fraction of pores falling within any 10 μm radius interval. It is not possible to plot the void fraction directly vs a constant Δr, for the reason discussed above. However, we can obtain such a plot from Fig. 2a, if we divide the void fraction corresponding to each step of the histogram by its radius interval width. If this width is greater than 1 μm, this procedure has the effect of lowering the step height, while the height is increased if Δr is less than 1 μm.

Fig. 2b, the result of treating Fig. 2a by the above procedure, is a histogram with a constant radius interval width of 1 μm. For example, the plot shows that approximately 1% of the pores have a radius of 25 ± 0.5 μm. The approximate void fraction of pores having radii between 50 and 100 μm could be found either by (a) integrating the area under that portion of the histogram and dividing by the total area of the

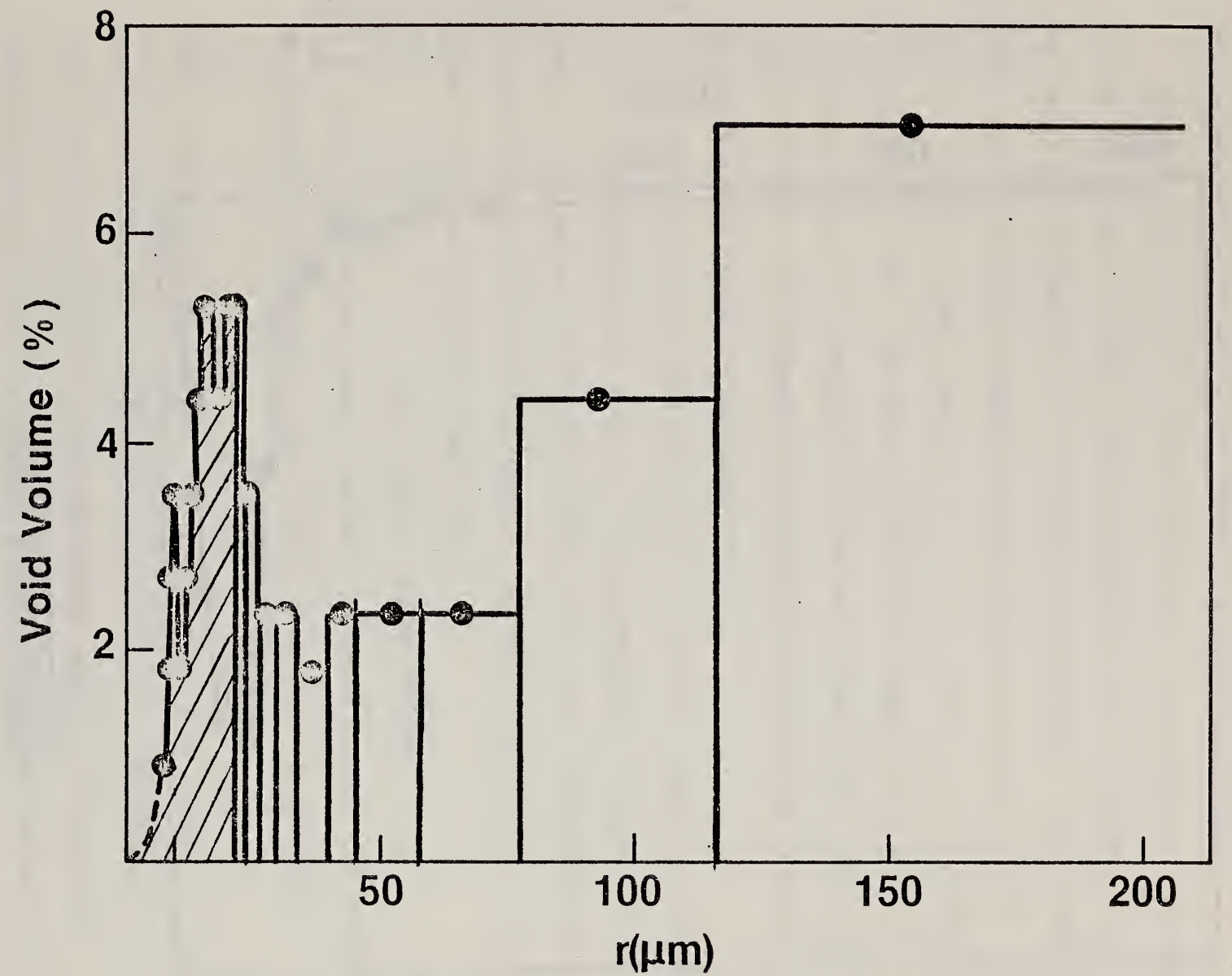

Figure 2a. Volume-weighted pore size histogram for one sample of PTFE-C composite. Pressure increment corresponding to each step of the graph is 0.5 psi . Shaded area consists of steps too small to resolve.

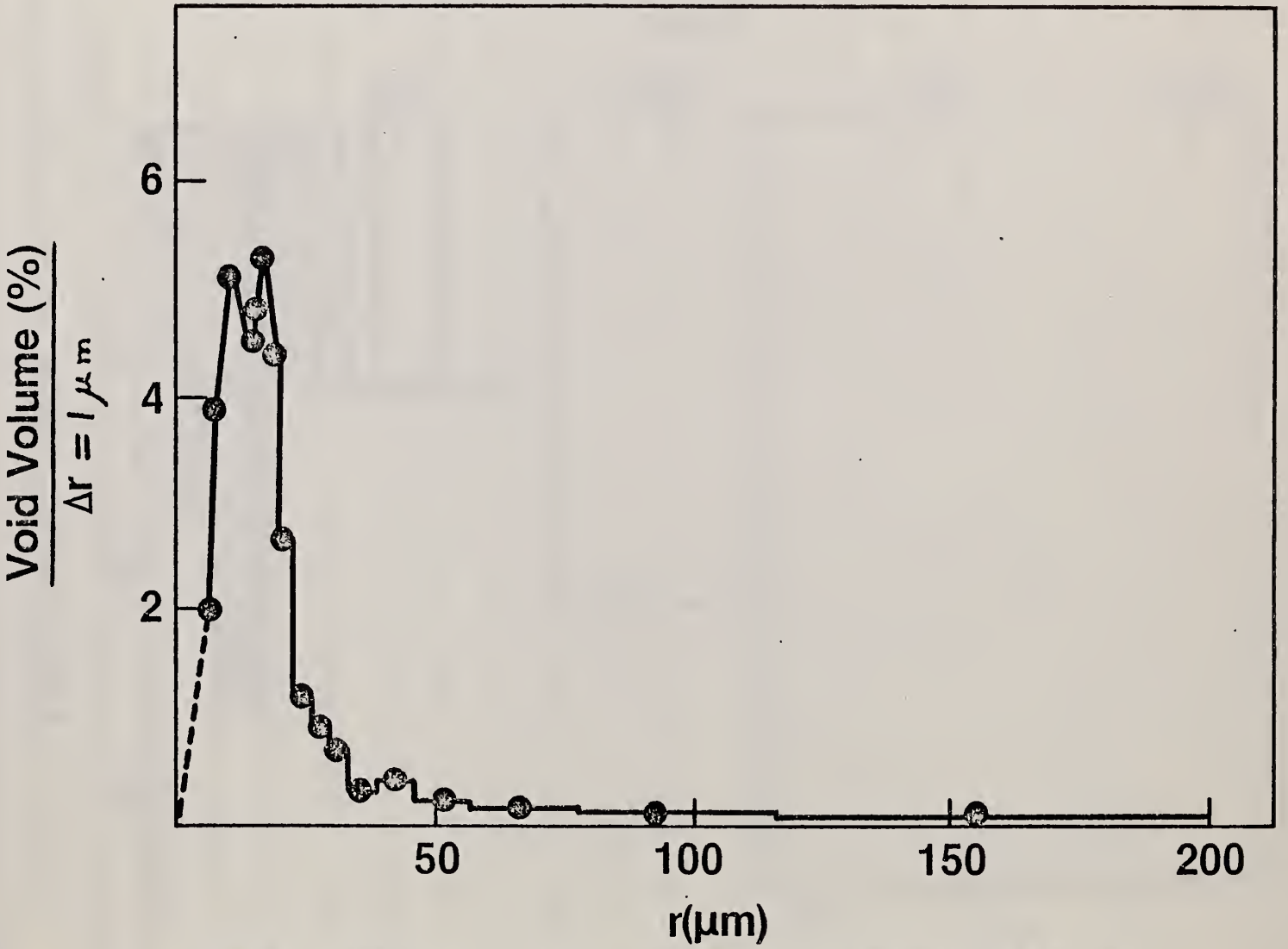

Figure 2b. Normalized plot of Fig. 2a, formed by dividing each void fraction step in 2a by its radius interval width. The vertical lines in the histogram are omitted for clarity.

histogram, or (b) adding together the void fractions, as read on the y-axis, corresponding to each 1 μm interval between 50 and 100 μm.

While the data are not sufficiently precise, particularly near the ends of the curve, to reveal the exact shape of this normalized plot, it has the general appearance of a log-normal distribution, a type which is often found for particles, metal grains, and other systems in which there is a definite lower limit to the size (in this case r = 0) but no definite upper limit. The curve is definitely skewed to the right of the "most probable" r represented by the peak of the curve. The distribution function is not symmetric about its maximum value as it would be, for example, for a normal (Gaussian) curve.

Figs. 3a and 3b are replots of Figs. 2a and 2b, formed by increasing the ΔP interval to 1 psi. Fig. 4 is an unnormalized histogram for one sample of the porous polyethylene, using ΔP = 1 psi. As compared with the corresponding plot for the composite material (Fig. 3a), it illustrates the much narrower pore size range of PPE.

IV. PORE SIZE BY BET METHOD

In our last Annual Report[2], we have described a method for measuring the average pore size based upon a simple geometrical relationship,

$$D = kV/S,$$

where D is the pore "diameter", V is the specific pore volume, S is the specific surface area, which we measured by the BET method, and k is a "shape factor" which varies with the assumed geometry of the pores. For spherical pores, k=6, and we used this factor to compare the pore sizes of the 2 implant materials. As compared with mercury porosimetry values for the average pore "diameter", based upon cylindrical pore shapes, the BET method yielded a pore diameter which was about twice the mercury intrusion value for PPE, and about half the mercury value for the composite.

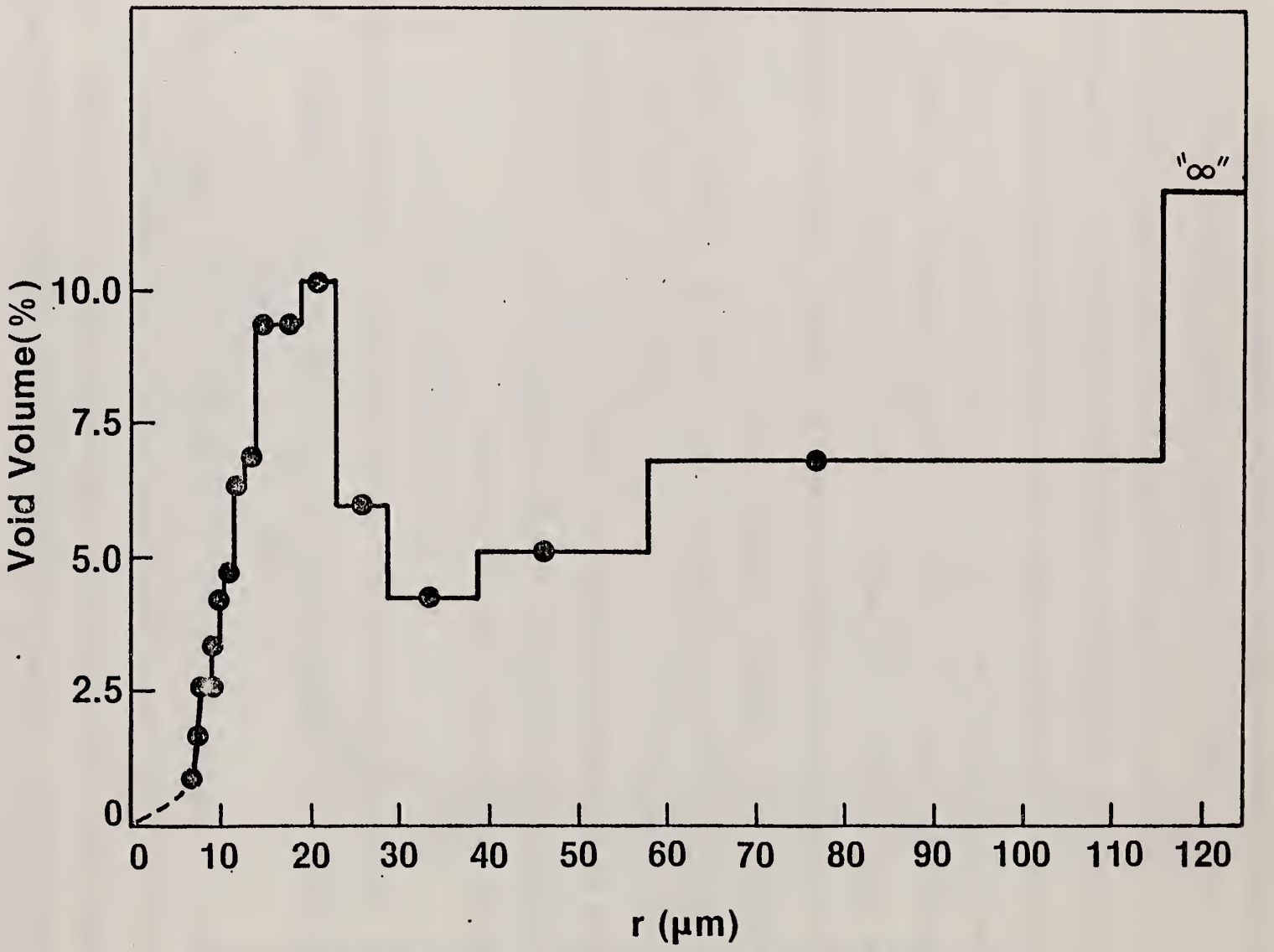

Figure 3a. Volume-weighted pore size histogram for same sample of PTFE-C composite as Fig. 2a. Pressure increment is 1.0 psi . Vertical lines are omitted.

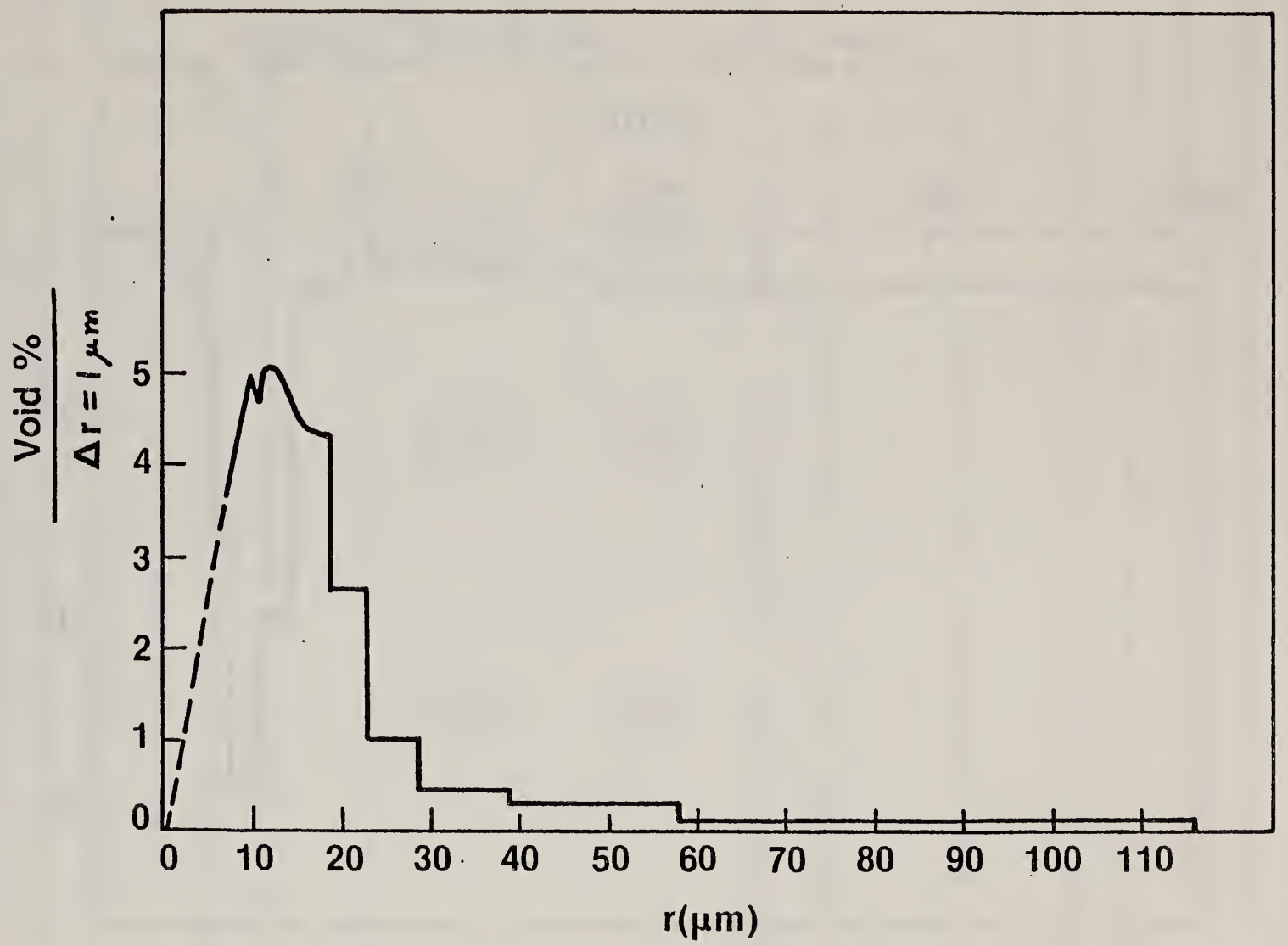

Figure 3b. Normalized plot of Fig. 3a.

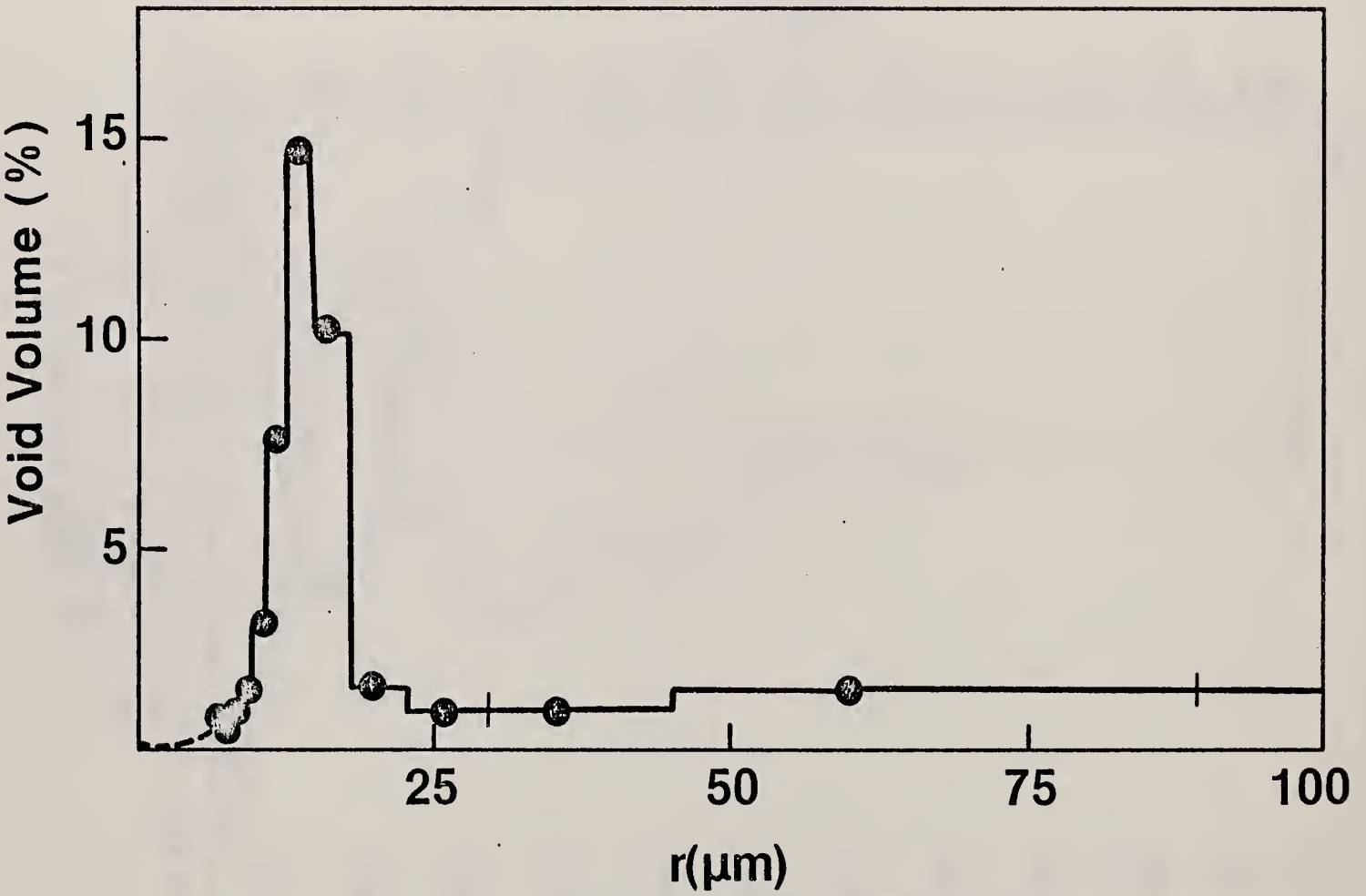

Figure 4. Volume-weighted pore size histogram for one sample of porous polyethylene. Pressure increment is 1.0 psi . Vertical lines are omitted.

The reason for these discrepancies was not readily apparent, but since we had analyzed only one sample of each material by the BET method, it was clearly necessary to confirm these results with more BET data.

During the current reporting period, we have analyzed 3 more samples of the composite and 2 more of the PPE by the BET method at a commercial laboratory[12].

The results of all 7 analyses to date are presented in Table 2.

Table 2. BET Surface Area Measurements for Two Porous Implant Materials

Sample	Wgt.(g)	Surface Area (m^2)	Specific Surface Area (m^2/g)
PPE			
	0.5091	0.0425	0.083
	0.2818	0.0235	0.083
	0.2680	0.0213	0.080
PTFE-C Composite			
(block)	0.6869	0.271	0.39
	0.4931	0.221	0.45
	0.5156	0.258	0.50
(sheet)	0.0730	0.0368	0.50

These sample sizes are not large enough to be subjected to statistical analysis. However, the consistency of these data indicates that our initially reported values, the first listed for each material in Table 2, were approximately correct. For the composite, the initial value of S may have been somewhat low, according to Table 2, but if we use a higher value we calculate an even lower value for D, which was already much lower than the mercury porosimetry value. It is apparent

even from these few BET measurements that the discrepancy between pore diameters as determined by the mercury intrusion and BET methods cannot be explained by faulty BET data.

V. COMPARISON OF POROSITY MEASUREMENT METHODS

While the amount of data which we have obtained to date is insufficient to permit statistically well founded comparisons of the accuracy and precision of the various methods of porosity measurement, certain tentative conclusions can be drawn on the basis of our current data. These are discussed in the following sections.

A. Pore Volume

On page 9 of our last Annual Report[2], we reported the pore volume fraction in PPE as obtained by the "apparent density" and mercury intrusion methods. The 2 methods yielded void volume fractions of 0.44 - 0.45 and 0.44, respectively. Our preliminary measurements by the optical microscopic technique, as reported above yielded 0.48 and 0.46 for the 2 sets of photographs, with standard deviations of 0.09 and 0.07. From these data, we conclude that there is little if any significant difference between the 3 different methods in their estimation of the pore volume. Indeed, if we assume that essentially all of the pores are interconnected, with no included voids, the 3 methods should give the same answer, and our results seem to confirm this expectation.

These preliminary results are quite encouraging. If, for example, the PPE samples were in some way distorted during preparation for optical microscopy, one might expect that the measured volume fraction would be affected. The good agreement which we find among the 3 methods reinforces our confidence in each one.

The BET method does not measure pore volume and therefore cannot be compared with the other methods.

B. Pore Size

We first recall that "size" is not a well defined physical property of an object until we arbitrarily give it meaning in terms of some measurable quantity. In the mercury intrusion method, "size" was defined as the diameter of an assumed cylindrical pore shape pertaining to interconnecting pores in the matrix. In the optical microscopy work, we have arbitrarily defined "size" as the mean intercept length. Other arbitrary definitions such as the mean or maximum tangent diameter could have been chosen equally well, but we have selected a measurement which appeared to be relatively simple as well as having a low probability of introducing operator bias.

As we have reported for PPE[2], the mercury intrusion method indicates that most (~80%) of the interconnecting pore "diameters" lie in the range 20-40 μm. Our optically measured mean intercept length, reported above, is about 75 μm or about twice the mercury intrusion "diameter". If we correct this $\bar{L}$ for the "sectioning" effect discussed in Section IIB above, the number is increased by the factor $(4/\pi)^2$ to about 120 μm, which is much greater than the "diameter" found by mercury intrusion. Certainly, the interconnecting pores measured by mercury intrusion are expected to be smaller than the "true" average pore size, although one might be somewhat surprised at the magnitude of the difference reported above. It must be remembered that our choice of the parameter to be measured by optical image analysis was arbitrary. A different choice might well have led to quite different conclusions than we have found by our chosen method.

The usefulness of any analytical technique depends in large part upon its ability to yield reliable data in a reasonable time and with a minimum of operator effort or judgment. In these respects, mercury porosimetry appears to have a clear advantage over image analysis methods, particularly if one is restricted to manual analysis. It requires no sample preparation and, if the instrument is working properly, yields a great deal of information about the pore size distribution with a single pressure-volume plot. Optical image analysis requires a much greater amount of operator time to give a statistically meaningful estimate of either pore size or pore volume. Furthermore, there is apparently no simple or rapid way to determine the pore size distribution by optical methods, whereas the mercury intrusion method provides at least semi-quantitative information about the distribution very quickly.

The BET method of measuring pore "size", discussed above and in our last Annual Report[2], is a hybrid method involving a surface area measurement, a pore volume measurement, and an assumed pore geometry in order to determine the average pore "diameter". The assumed pore shape can have a considerable effect on the calculated pore "diameter", and, as we have discussed before, one has no reason to choose any particular pore geometry over another for irregularly shaped pores. Our experience does indicate that both surface area and pore volume can be estimated fairly precisely with very few measurements. In this respect, the BET method appears to have an advantage over image analysis methods. Like the latter, however, the BET method gives no information about the pore size distribution.

C. Summary Table

1. Mercury Porosimetry

Advantages

- relatively little operator time required for each measurement
- no sample preparation required
- no operator judgment required
- gives pore size distribution rather than just an average value
- gives much information in a single P-V plot
- capable of measuring smaller pores than is possible by optical techniques at high Hg pressure, though advantage not needed for pores in implant materials

Disadvantages

- gives interconnecting rather than "true" pore diameters
- requires assumed pore shape to interpret the data
- only 2 or 3 PV plots obtainable per day, due to long vacuum pump-down time
- sensitivity poor for large pores

2. Optical Image Analysis

Advantages

- little operator judgment required
- gives "true" pore size, rather than interconnecting pore size
- sensitivity equally good for large and small pores, but minimum measurable size limited by chosen magnification

Disadvantages

- sample preparation can be difficult and time consuming
- sample preparation may alter the porosity

- may be difficult to obtain good phase contrast
- difficult to obtain information about distribution of pore sizes
- many measurements needed to obtain statistically meaningful results

3. BET Method

Advantages

- both surface area and pore volume can be estimated well with few measurements
- more rapid than optical image analysis
- no sample preparation required
- gives "true" pore size rather than interconnecting pore size

Disadvantages

- requires assumed pore shape to calculate pore "diameter"
- does not give pore size distribution
- surface area measurement may be subject to unknown systematic errors

VI. MECHANICAL PROPERTIES OF POROUS IMPLANT MATERIALS

One item in our work plan for the current year requested a range of pressures which can safely be applied to PPE and the PTFE-C composite without distorting the materials. This information is important not only in determining whether the materials would be expected to deform significantly during a mercury intrusion experiment, but also in suggesting the degree of care which should be exercised by clinical workers in handling the materials prior to and during implantation. In order to answer these questions, we have performed compressive stress-strain measurements on the porous implant materials using our Instron® universal testing machine.

A. Experimental

Small, rectangular specimens of PPE and PTFE-C composite were cut from blocks of these materials with a fresh scalpel. For the composite, samples were cut in 2 ways, with the laminar planes parallel or perpendicular to the area of applied stress. Sample dimensions were measured with precision calipers. The crosshead speed of the instrument was 0.02 in/min (0.05 cm/min), and the maximum resolution of the stress measurement was 10 g per division of chart paper, with a 1 Kg full scale stress.

B. Results

Figure 5 shows the stress (σ) vs. strain (ε) plots obtained for 2 samples of PPE. The curves are parallel, except for their initial compression moduli ($\Delta\sigma/\Delta\varepsilon$), which differ by about a factor of 2, up to 4% strain. The bottom curve is somewhat suspect due to its rather abrupt change in slope at about 10kg/cm^2 (1.01 x 10^6 Pa). It is probable that the initial compression modulus was higher than our assumed value for this curve, due to the fact that the initial area of applied stress was smaller than our measured area, so that our calculated stress was too low. Using only hand tools, it was not always possible to cut the top and bottom stress areas exactly parallel, as they should be for proper sample alignment. In such a case, the two opposing stress areas were soon forced into parallel alignment by the descending crosshead of the instrument, so that the curves in Figure 5 are parallel for ε greater than about 0.05.

As expected, the strain resulting from 1 atmosphere stress (1 kg/cm^2, 1.01 x 10^5 Pa) was very small (<1%) for PPE. To induce a 1% strain in this material, a pressure of about 10 kg/cm^2 was required according to the top curve in Figure 5. We also observe that this

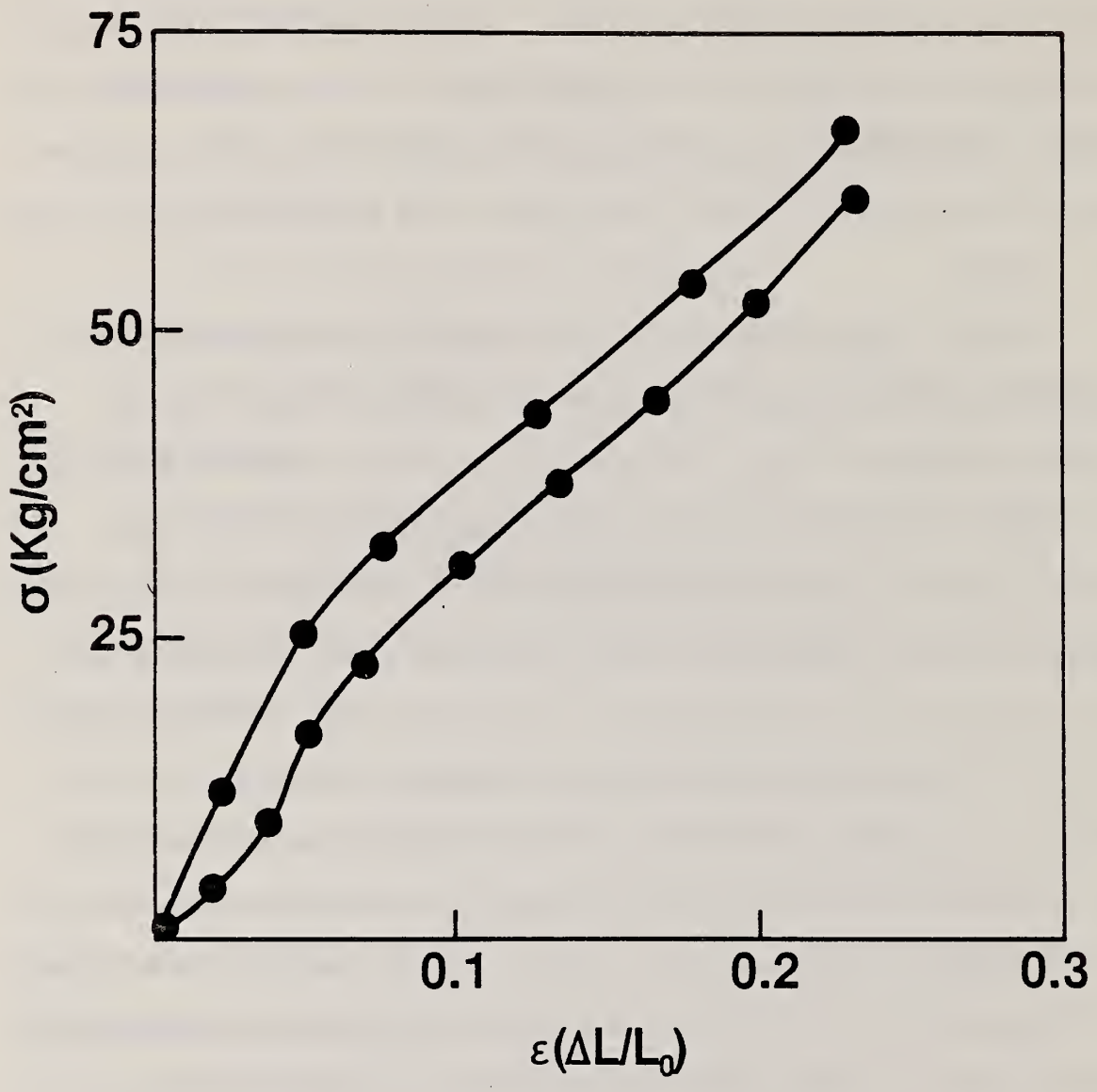

Figure 5. Compressive stress-strain curves for 2 samples of porous polyethylene.

material had an approximately constant compression modulus (i.e., it was elastically compressed) up to a pressure of 25-30 kg/cm^2, corresponding to about 5% strain. Above 30 kg/cm^2, the material became slightly more compressible and retained this smaller modulus up to the highest applied pressure, 66 kg/cm^2.

Figure 6 shows stress-strain plots for 4 samples of the PTFE-C composite. As noted on the figure, 2 of the samples were stressed parallel to the laminar planes and 2 were stressed perpendicular to the laminae. The plots clearly illustrate the mechanical anisotropy of this material. The compression modulus was much higher for parallel stress, because the laminar planes stiffen the material with respect to compression in this direction. Elastic compression occurred up to about 5-7% strain, after which the modulus began to decrease, passed through 0, and became negative at about 10% strain. These phenomena resulted from the bending of the sample as the pressure was increased, so that the applied force was no longer exactly parallel to the laminar planes. The material thus became more easily compressed as the bending continued. The difference between the 2 curves for parallel compression is greater than the difference for the 2 perpendicular compression curves due to the fact that sample alignment with respect to the crosshead was more critical in the parallel direction, and we did not have a very precise method for adjusting this alignment. Following this reasoning, we assume that the curve displaying the higher initial compression modulus represented the better alignment, because the modulus should be greatest when the laminar planes are exactly parallel to the applied stress.

When the sample was compressed perpendicular to the laminar planes,

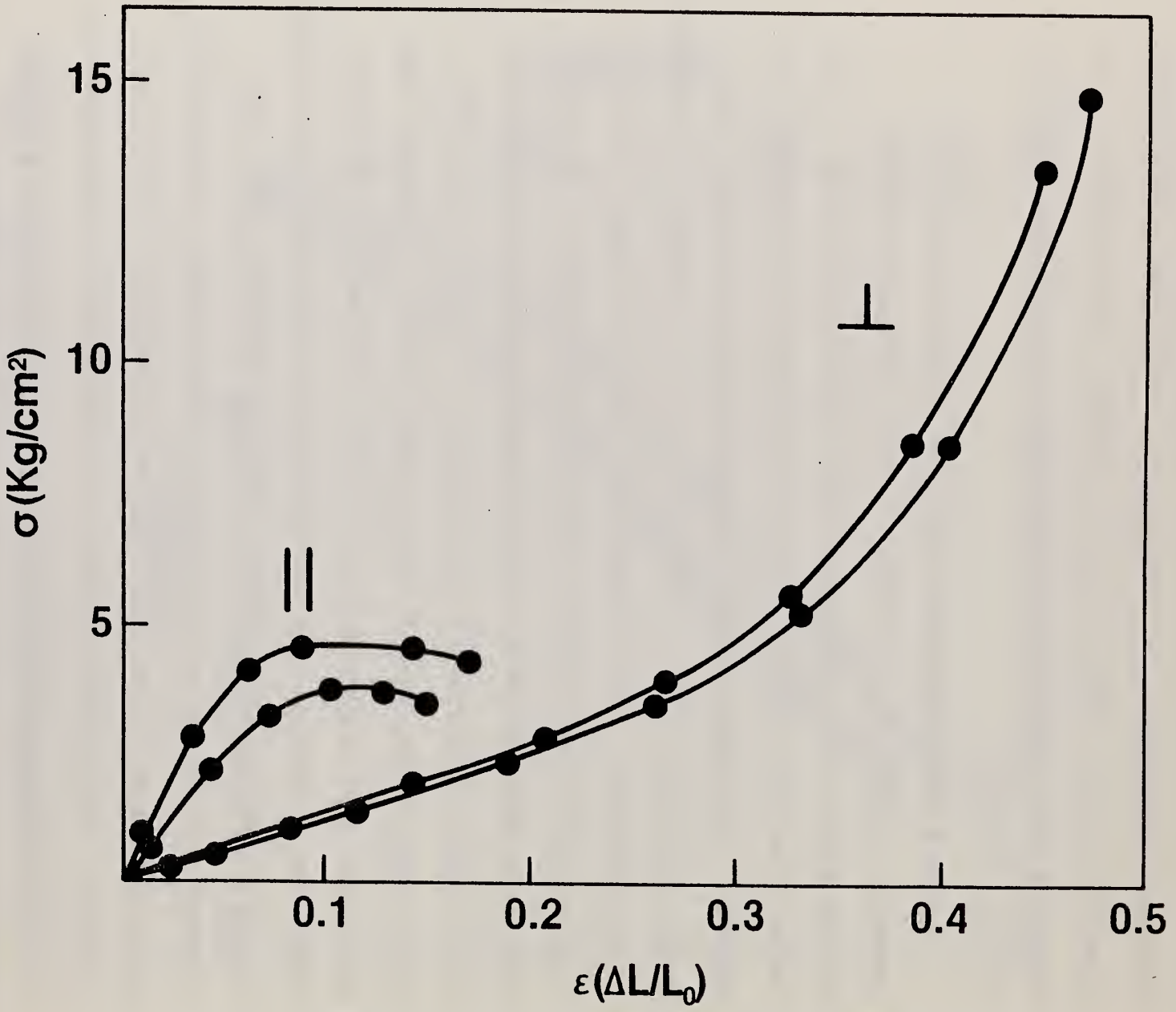

Fig. 6. Compressive stress-strain curves for 4 samples of PTFE-C composite. Two samples aligned parallel (‖) and perpendicular (⊥) to applied stress

its initial modulus was only about 1/6 that in the parallel direction. However, unlike parallel compression, the modulus increased monotonically with increasing stress, above about 2.5 kg/cm^2. A pressure of 1 atmosphere (1 kg/cm^2), the maximum applied during a mercury intrusion experiment, induced about 8-9% strain. This compression was not entirely elastic, as we learned by increasing the stress to 1 atmosphere, releasing the stress, and recycling to 1 atmosphere. If this compression were entirely elastic, the stress-strain curve would be reproducible and independent of the number of previous compression cycles. However, each time we repeated this compression cycle, the modulus increased (by diminishing amounts), indicating increasing inelastic deformation of the material.

C. Implications for Mercury Porosimetry

It is important to decide whether the small strain induced in the composite material at 1 atmosphere pressure should be considered a deterrent to the use of mercury porosimetry in studying this material. While any amount of compression is undesirable, we recall that 1 atmosphere was the highest pressure applied during the mercury intrusion experiment, and it corresponds to a pore size smaller than that generally thought to be optimum for tissue ingrowth. Less than 0.5 atmosphere pressure is required to measure pores larger than about 30 μm in diameter, and our stress-strain plots indicate that this stress induces only about 5% strain in the material. For pores 80 μm in diameter, only 0.2 atmosphere pressure is required, and this corresponds to a strain of only about 2%. Thus, the strain induced in this material is small over the pressure range corresponding to pores large enough for tissue ingrowth. Furthermore, as the mercury begins to enter the pores at low pressure, one might expect the compression modulus to increase somewhat, due to

the stiffening effect of the intruding liquid, so that our stress-strain measurements in air may overestimate the actual strains induced during mercury intrusion.

Taken all together, these observations indicate that the pressures necessary to measure the pores of interest in the PTFE-C composite by mercury porosimetry are not likely to introduce more than very small errors due to bulk compression of the material.

VII. SURFACE AREA BY MERCURY POROSIMETRY

A. Theory

In addition to the well known BET method for measuring the surface area of porous materials, which we have discussed above, there are other methods available as well for measuring this quantity. One which is particularly pertinent to our current work involves the use of mercury porosimetry data[13]. It rests upon the same assumptions that were used to determine pore "diameters" from mercury intrusion data. As in the latter, the usual assumption is that the pores are cylindrical in shape, because the calculation can be done exactly for this pore geometry.

Work is required to force mercury into a cylindrical pore. The amount of work is proportional to the surface tension of mercury (γ) and to the increase in surface area of mercury which is created when it is forced into the pores. This work (W) is as given by the equation

$$W = 2\pi r l \gamma \cos\theta \qquad (7)$$

where r and l are the radius and length of the pore and θ is the contact angle of mercury on the surface of interest. The factor cos θ represents a reduction in the work required; it is of course maximum for θ = 0° or 180°, corresponding to a hemispherical meniscus. Figure 7 illustrates the way a liquid behaves in a capillary when θ<90° (a), θ>90° (b),

and $\theta = 90°$ (c). Mercury, which is "non-wetting" on most surfaces, corresponds to case (b). Case (c) would result if the liquid did not form a meniscus. Physically this situation means that the energy of the liquid-solid interaction is identical to the interaction of the liquid with itself, so that no additional energy is gained or lost when the liquid contacts the solid surface.

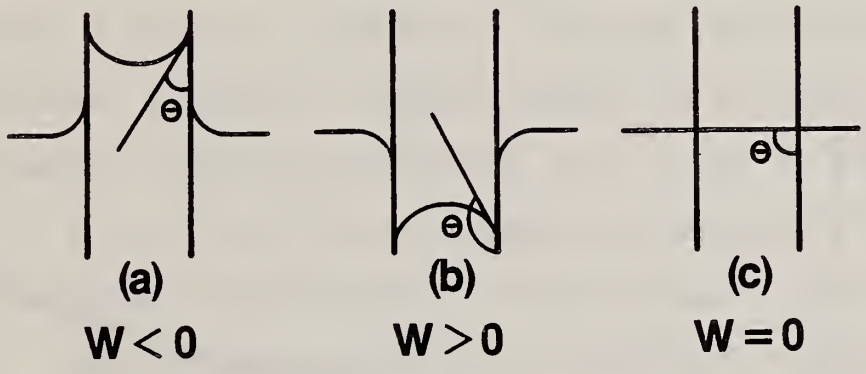

Figure 7. Relationship of Solid-Liquid Contact Angle to the Work of Forming a Meniscus.

The work of forcing mercury into a cylindrical pore can also be related to the pressure (P) and volume increment (ΔV) of the intruding mercury according to the equation

$$W = P\Delta V = P\pi r^2 l. \tag{8}$$

Equating (7) and (8), we obtain the familiar Washburn equation,

$$2\pi rl\gamma|\cos\theta| = P\pi r^2 l, \tag{9}$$

or

$$Pr = 2\gamma|\cos\theta|. \tag{10}$$

(Cos θ must be taken as a positive quantity because all other terms are positive). From Eqs. 8 and 9 we can also form the equality

$$P\Delta V = 2\pi r l \gamma |\cos\theta| . \qquad (11)$$

Since $2\pi rl$ is the surface area (S) of a cylindrical pore, Eq. 11 may be written

$$P\Delta V = S\gamma |\cos\theta| . \qquad (12)$$

This may also be written as a differential equation,

$$PdV = dS\gamma |\cos\theta| ,$$

or

$$dS = PdV/\gamma |\cos\theta| .$$

Integrating, we find

$$S = 1/\gamma |\cos\theta| \int_{o}^{V} PdV \qquad (13)$$

Equation 13 provides the basis for using mercury porosimetry data to obtain the surface area of a porous material. Instead of plotting the mercury volume V vs. log P, as is customary in the usual plot used to obtain pore size information, we make a linear plot of V vs. P. A typical such plot is shown in Fig. 8 , with the shaded area to be integrated. We used a mechanical planimeter to perform these integrations.

When S is divided by the sample weight, one obtains the specific surface area which, in combination with the specific void volume of the material, may be used to estimate the average pore size in the test sample. This is the same procedure as our BET method, except for the different method of determining S.

B. Results

In Table 3, we summarize the results of 4 specific surface area determinations by the method outlined above, together with the BET results reported in Section IV.

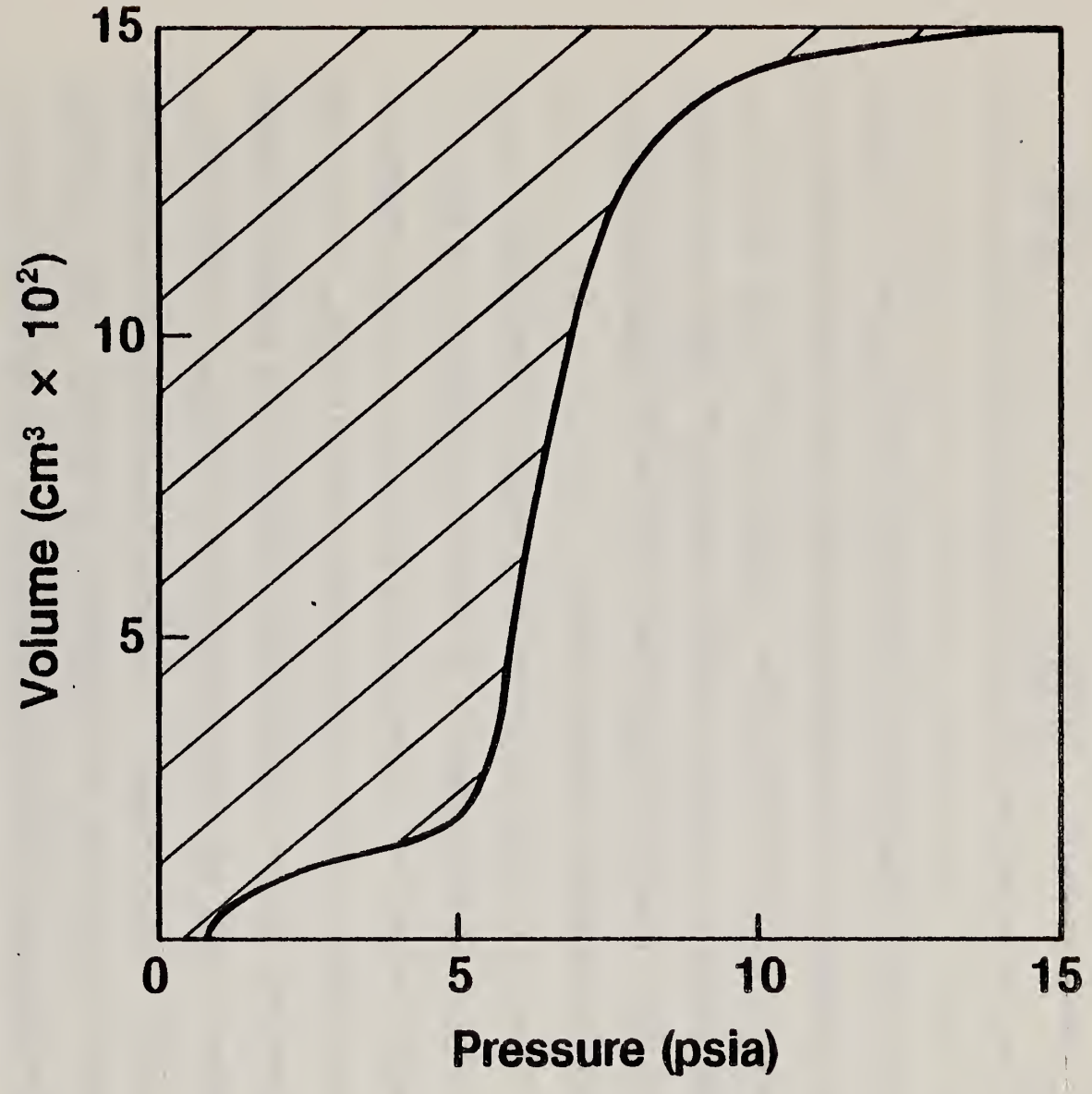

Figure 8. Linear plot of V vs. P obtained by mercury porosimetry for porous polyethylene. Surface area proportional to integrated shaded area.

Table 3. Specific Surface Area (m^2/g) Determined by Two Different Methods

	BET	Mercury Intrusion
PPE	0.082 (av. of 3)	0.125
PTFE-C (block)	0.45 (av. of 3)	0.192
PTFE-C (sheet)	0.50 (1 only)	0.171 0.173

While these results must be considered tentative, due to the small number of samples, certain trends are evident even from these few data. The mercury intrusion method yields a specific surface area which is probably somewhat larger than the BET value for PPE, while the results for the PTFE-C composite are reversed, with the BET value probably at least twice the mercury intrusion value.

C. Comparison of Pore Size by Two Surface-Pore Volume Methods

In our last Annual Report[2], on page 25, we discussed the pore "diameters" determined for both implant materials by the BET method using the formula D = 6V/S, which assumes spherical pores, to calculate the diameters. For PPE and the PTFE-C composite, the average "diameters" determined in this way were found to be 61 μm and 25 μm, respectively. If we correct the diameter of the composite's pores by using our current average BET surface area for 3 samples of the material, the calculated diameter decreases slightly from 25 to 22 μm. As compared with the average pore size determined by the direct mercury porosimetry method, using the Washburn equation, the BET method gave a larger value for PPE, by about a factor of two, while the value for the composite was only about half that obtained by the mercury intrusion method.

If we use the same factor 6V/S to determine the pore diameter, with S measured by the mercury intrusion method, the average diameter for PPE is found to be 40 μm, while the diameter for the composite is 52 μm. These values are to be compared with our reported values of 30 μm for PPE and 50 μm for the composite, as determined directly from analysis of the mercury intrusion P-V plot, using the Washburn equation.

It is not surprising that the two mercury intrusion methods, i.e., the direct method using the Washburn equation and the indirect method using the mercury intrusion surface area, agree so well in their determination of average pore diameter. Both use the same pressure-volume data, and both are constrained to the measurement of "interconnecting" pores in the matrix. This so-called "ink bottle" effect discussed in our last Annual Report causes the Washburn equation to underestimate the average pore diameter. It also overestimates the average pressure required to force mercury into the pores, because pressure and pore diameter are inversely related according to the Washburn equation. Therefore, when we measure surface area by integrating the pressure-volume plot, since the pressures are higher than the "true" pressures would be if the pores were indeed cylindrical in shape, we obtain a surface area which is larger than the true value. Since the pore diameter according to this method is proportional to V/S, and since S is overestimated, the diameter which we obtain is underestimated. In other words, both the direct and indirect methods of measuring pore diameter by mercury intrusion lead to an underestimation of pore diameter for the same reason.

Unfortunately, none of the above discussion reveals the reason why our BET surface area for the PTFE-C composite is larger than the area

determined by mercury porosimetry. Exactly the opposite would be expected if the BET method is considered to yield the "true" surface area. It is possible that the presence of finely divided carbon in the material could be responsible for this inconsistency, although it is difficult to predict exactly how this would affect the measurements. Certainly, finely divided particles can add a great deal to the surface area of a material but little to the volume, because the surface/volume ratio is inversely proportional to the radius of the particles. Perhaps mercury intrusion could change this surface area by pressing the fine particles against the larger PTFE particles, or perhaps the carbon tends to "float" ahead of the intruding mercury, since it is probably not bonded to PTFE. At present, however, we must conclude that the apparent inconsistency in surface area determinations between BET and mercury intrusion methods for the composite material is not well understood.

VIII. SUMMARY

The major accomplishments during the current reporting period may be summarized as follows:

(1) Quantitative Optical Microscopy

For porous polyethylene, we have developed a method for preparing samples for the stereological analysis which provided both the mechanical rigidity needed for grinding and polishing the material and the phase contrast necessary for performing quantitative measurements on photomicrographs of the material. The volume fraction of voids in the material was measured by the point count method, and the size of pores was measured by the mean intercept method, where the mean intercept length

$$\bar{L} = P_P/N_L.$$

We have reported a method for determining the number of measurements needed to obtain any desired degree of accuracy, given an initial estimation of the population mean and standard deviation.

According to the above, we have made preliminary measurements of the pore volume fraction and mean intercept length for filled PPE. The pore volume fraction (P_p) was found to be about 0.46 - 0.48, while $\bar{L}$ was found to be about 75 μm.

(2) Mercury Porosimetry

We have made plots of the volume-weighted pore size distribution from mercury porosimetry data, using interval lengths of r estimated by a random error analysis of the mercury intrusion experiment. These plots clearly show that the sensitivity of a mercury porosimeter as pore size measuring device increases rapidly with increasing pressure, and it is especially poor when the pore radius exceeds about 80 μm. When these plots were normalized to a constant radius interval length, they assumed the general appearance of a log-normal distribution, with the curve skewed to the right of the "most probable" radius.

(3) BET Pore Size Method

A total of 3 BET surface area measurements have been made for PPE, and 4 measurements for the composite material. The results indicate that our single values for each material reported in our last Annual Report were approximately correct. There remains the question of why the average pore size predicted by the BET-pore volume method is less than that found by mercury porosimetry for the composite material. Exactly the opposite is predicted from the fact that mercury porosimetry senses "interconnecting" rather than "true" pore diameters.

(4) Mechanical Properties

Compressive stress-strain measurements have been performed on both of the porous implant materials, using our Instron® machine. For PPE, the stress necessary to introduce 1% strain was about 10 kg/cm^2 (10 atmospheres), indicating that one may safely perform mercury intrusion experiments up to 1 atmosphere pressure with negligible deformation of the material. The PTFE-C composite in block form was quite anisotropic mechanically. When the stress was applied parallel to the laminar planes, the initial compression modulus was about 6 times that found for compression in the perpendicular direction. One atmosphere pressure induced about 8-9% strain in the latter direction.

(5) Surface Area by Mercury Porosimetry

In addition to the BET method, surface area may be measured independently by integration of pressure-volume plots obtained from mercury intrusion data. We have found that this method leads to a surface area for the PPE which is somewhat greater than that obtained by the BET method; the opposite is true for the composite, with the mercury intrusion value less than half that found by the BET method. The reasons for these discrepancies were not readily apparent.

A summary of the advantages and disadvantages of mercury porosimetry, optical image analysis, and the BET method is given in Section VC.

REFERENCES

1. Dehl, R. E., Grant, W. H., and Cassel, J. M., "Evaluation of Methods of Characterizing the Porosity of Porous Polymeric Implant Materials: A Review of the Current Status of Porosity Measurements", NBSIR 81-81-2212 (available from National Technical Information Service). Annual Report prepared for the Bureau of Medical Devices, Food and Drug Administration, Silver Spring, MD (February 1981).
2. Dehl, R. E., Grant, W. H., and Cassel, J. M., "Characterization of Porosity in Porous Polymeric Implant Materials", NBSIR 81-2459 (Available from National Technical Information Service). Annual Report Prepared for the Bureau of Medical Devices, Food and Drug Administration, Silver Spring, MD (February 1982).
3. Registered trademark of the Richards Manufacturing Company.
4. Registered trademark of Vitek, Inc.
5. DeHoff, R. I. and Rhines, F. N., "Quantitative Microscopy", McGraw-Hill, New York, 1968.
6. Underwood, E. E., "Quantitative Stereology", Addison-Wesley, Reading, MA, 1970.
7. Beddow, J. K. and Meloy, T., "Testing and Characterization of Powders and Fine Particles", Heyden, Philadelphia, PA, 1980.
8. Allen, T, "Particle Size Measurement", 3rd Ed., Chapman and Hall, New York, 1981.
9. Kaye, B. H., "Direct Characterization of Fine Particles", John Wiley and Sons, New York, 1981.
10. Castolite ^{TM} Resin, trademark of Buehler, Ltd.
11. Washburn, E. W.; Proc. Nat. Acad. Sci. 7, 115 (1921).
12. Quantachrome Corporation, Syosset, NY.
13. Lowell, S., "Introduction to Powder Surface Area", John Wiley and Sons, New York, 1979.

NBS-114A (REV. 2-80)

U.S. DEPT. OF COMM. BIBLIOGRAPHIC DATA SHEET (See instructions)	1. PUBLICATION OR REPORT NO. NBSIR 83-2645	2. Performing Organ. Report No.	3. Publication Date February 1983

4. TITLE AND SUBTITLE

Characterization of Porosity in Porous Polymeric Implant Materials

5. AUTHOR(S)
Ronald E. Dehl

6. PERFORMING ORGANIZATION (If joint or other than NBS, see instructions)

NATIONAL BUREAU OF STANDARDS
DEPARTMENT OF COMMERCE
WASHINGTON, D.C. 20234

7. Contract/Grant No.

8. Type of Report & Period Covered

9. SPONSORING ORGANIZATION NAME AND COMPLETE ADDRESS (Street, City, State, ZIP)

Bureau of Medical Devices
Food and Drug Administration
Silver Spring, MD 20910

10. SUPPLEMENTARY NOTES

☐ Document describes a computer program; SF-185, FIPS Software Summary, is attached.

11. ABSTRACT (A 200-word or less factual summary of most significant information. If document includes a significant bibliography or literature survey, mention it here)

In this report, we describe (1) the continued exploration of methods for characterizing the porosity of two commercial implant materials, a porous polyethylene and a composite of polytetrafluoroethylene and carbon, and (2) the compressive stress-strain behavior of these materials. A major emphasis was placed upon optical image analysis of porous polyethylene. The pore volume fraction obtained from analysis of 20 photomicrographs (0.47) agreed well with the fraction previously found by two other methods. The mean intercept length, determined from the same photomicrographs, was about 75 μm, a value considerably higher than the average "interconnecting" pore diameter determined by mercury porosimetry (30 μm). Replotting our mercury porosimetry data, we found that the volume-weighted pore size distribution curve resembled a log-normal distribution, skewed to the right of the "most probable" pore radius. The surface area determined from mercury porosimetry data was somewhat larger (0.125 m^2/g) for the porous polyethylene than that determined by the BET method (0.082 m^2/g), while the reverse was true for the composite material (0.19 vs 0.45 m^2/g). Compressive stress-strain measurements on the laminated composite demonstrated that the initial compression modulus is approximately six times greater when the stress is applied parallel rather than perpendicular to the laminar planes.

12. KEY WORDS (Six to twelve entries; alphabetical order; capitalize only proper names; and separate key words by semicolons)

Pore size; pore volume; porous implants; porous polyethylene; PTFE-carbon composite; stereology; stress-strain plots; surface area.

13. AVAILABILITY

☒ Unlimited

☐ For Official Distribution. Do Not Release to NTIS

☐ Order From Superintendent of Documents, U.S. Government Printing Office, Washington, D.C. 20402.

☒ Order From National Technical Information Service (NTIS), Springfield, VA. 22161

14. NO. OF PRINTED PAGES
51

15. Price
$10.00

USCOMM-DC 6043-P80